CORRIGENDUM

Development 137, 2603 (2010) doi:10.1242/dev.055913

Ovo1 links Wnt signaling with N-cadherin localization during neural crest migration

Sarah Piloto and Thomas F. Schilling

There was an error published in *Development* **137**, 1981-1990.

On p. 1983, the GEO accession for the microarray data should read GSE21539.

The authors apologise to readers for this error.

Development 137, 1981-1990 (2010) doi:10.1242/dev.048439

Ovo1 links Wnt signaling with N-cadherin localization during neural crest migration

Sarah Piloto and Thomas F. Schilling*

SUMMARY

A fundamental issue in cell biology is how migratory cell behaviors are controlled by dynamically regulated cell adhesion. Vertebrate neural crest (NC) cells rapidly alter cadherin expression and localization at the cell surface during migration. Secreted Wnts induce some of these changes in NC adhesion and also promote specification of NC-derived pigment cells. Here, we show that the zebrafish transcription factor Ovo1 is a Wnt target gene that controls migration of pigment precursors by regulating the intracellular movements of N-cadherin (Ncad). Ovo1 genetically interacts with Ncad and its depletion causes Ncad to accumulate inside cells. Ovo1-deficient embryos strongly upregulate factors involved in intracellular trafficking, including several *rab GTPases*, known to modulate cellular localization of cadherins. Surprisingly, NC cells express high levels of many of these *rab* genes in the early embryo, chemical inhibitors of Rab functions rescue NC development in Ovo1-deficient embryos and overexpression of a Rab-interacting protein leads to similar defects in NC migration. These results suggest that Ovo proteins link Wnt signaling to intracellular trafficking pathways that localize Ncad in NC cells and allow them to migrate. Similar processes probably occur in other cell types in which Wnt signaling promotes migration.

KEY WORDS: Neural crest, N-cadherin, Wnt, Zebrafish

INTRODUCTION

Migratory cells must dynamically regulate adhesion as they move. Neural crest (NC) cells in vertebrate embryos are highly migratory progenitor cells that form diverse cell types including cartilage and bone of the skull, sensory neurons and glia of the peripheral nervous system, and pigment cells of the skin (Le Douarin et al., 2004). These cells actively regulate expression of cadherins on their surfaces as they delaminate and migrate from the dorsolateral edges of the neural tube (Monier-Gavelle and Duband, 1995; Nakagawa and Takeichi, 1995; Nakagawa and Takeichi, 1998). Members of the Wnt family of secreted signals induce NC cells to initiate migration but their roles in cadherin regulation and morphogenesis are largely unknown.

NC precursors in the neural ectoderm initially express both Cadherin 6b (Cad6b) and N-cadherin (Ncad; Cdh2 – Zebrafish Information Network), but downregulate both and upregulate Cadherin7 (Cad7) as they undergo an epithelial-mesenchymal transition (EMT) and begin to migrate (Nakagawa and Takeichi, 1995; Akitaya and Bronner-Fraser, 1992). Functions for individual cadherins in this process remain unclear. For example, either increasing or decreasing Ncad protein levels disrupts NC cell migration in avian embryos (Nakagawa and Takeichi, 1998). Also, overexpressing full-length Ncad inhibits NC migration, whereas a truncated version translocates to the nucleus and promotes cell cycle progression and EMT in response to Bmp signaling (Shoval et al., 2007). *Ncad*$^{-/-}$ mutant NC cells in mice migrate in inappropriate directions (Xu et al., 2001), whereas defects in neural tube closure (but not in NC) have been reported in *ncad*$^{-/-}$ mutant zebrafish (Lele et al., 2002).

NC cells establish transient cell-cell contacts during migration, possibly by regulating Ncad localization to their filopodial tips (Monier-Gavelle and Duband, 1995). But how is this localization regulated? Members of the Rab family of GTPases are attractive candidates. Rab11-mediated recycling of *Drosophila* Ecad regulates cell intercalation during tracheal morphogenesis in response to Wnt signaling (Shaye et al., 2008). Interestingly, this regulation of cell adhesion is mediated by Spalt, a Wnt-responsive transcription factor (Shaye et al., 2008). These studies suggest roles for intracellular trafficking in cadherin localization and cell migration through tissue-specific transcriptional control in response to Wnt signaling.

Wnt signaling not only induces EMT in NC cells but also specifies NC lineages that give rise to pigment cells (Dorsky et al., 1998). In zebrafish, single NC cells labeled adjacent to the neural tube give rise to clones of progeny that are lineally restricted to single cell types (e.g. skeletal, neural, pigment), suggesting that fates are specified prior to migration (Schilling and Kimmel, 1994; Raible et al., 1994). Overexpression of a truncated, dominant-negative form of Tcf3 (dnTcf3) in individual NC cells inhibits pigment cell formation, whereas an activated form of β-catenin (βcat; Ctnnb – Zebrafish Information Network) promotes pigment cell fates (Dorsky et al., 1998). Wnt signaling also directly promotes *mitfa* expression, a key regulator of melanocytes (Dorsky et al., 2000). Wnt3a added to chick NC explants increases melanocyte number (Jin et al., 2001), whereas *Wnt1*$^{-/-}$*/Wnt3a*$^{-/-}$ double-mutant mice form fewer melanoblasts and NC cells in general (Ikeya et al., 1997). Interestingly, Wnt signals regulate NC cell EMT, at least in the trunk, by controlling *cyclin D* expression and cell cycle progression (Burstyn-Cohen and Kalcheim, 2002; Burstyn-Cohen et al., 2004). Wnts also activate *snail* transcription

Department of Developmental and Cell Biology, University of California, Irvine, CA 92697-2300, USA.

*Author for correspondence (tschilli@uci.edu)

Accepted 7 April 2010

factors, well-known transcriptional repressors of E-cadherin (Ecad; Cdh1 – Zebrafish Information Network) and Cad6b, providing a possible direct link between Wnt functions in cell fate determination and adhesion (Aybar et al., 2003; Cano et al., 2000; Taneyhill et al., 2007; Vallin et al., 2001).

In addition to *snail*, Wnt signaling also regulates expression of other zinc finger transcription factors, including members of the evolutionarily conserved family of *Ovo* genes (Dai et al., 1998; Mackay et al., 2006; Mevel-Ninio et al., 1991; Oliver et al., 1994). Drosophila *ovo* is a direct Wnt target involved in germline development and epidermal appendage formation (Khila et al., 2003; Mevel-Ninio et al., 1991; Payre et al., 1999). Mice have three *Ovo-like* (*Ovol*) genes, *Ovol1-3*, and *Ovol1* is a Wnt target in the mammalian germline and epidermis (Dai et al., 1998; Li et al., 2002). By contrast, *Ovol2* is required for neurulation and cranial NC migration; a subset of NC cells remains attached to the neural tube in *Ovol2* mutant mice (Mackay et al., 2006). However, whether or not this reflects a role for Ovo downstream of Wnt proteins or in controlling NC cell adhesion and fate remains unclear.

Here we report the characterization of zebrafish *ovo1* and show that it is a Wnt target that controls NC migration, in part by regulating intracellular trafficking of Ncad. Depletion of Ovo1 in vivo causes a subset of NC cells to cluster in the dorsal midline above the neural tube. Ovo1 genetically interacts with Ncad and promotes its membrane localization. One possible mechanism is through inhibition of *rab* expression. *rab* overexpression accounts for at least part of the NC defects in Ovo1 morphants as (1) a chemical inhibitor of Rab function rescues the morphant phenotype, and (2) misexpression of a *rab11*-interacting factor causes similar NC migration defects. These data suggest that Ovo1 links Wnt signaling to changes in NC cell adhesion by regulating Ncad localization to the membrane, which has important consequences for subsequent NC cell fates.

MATERIALS AND METHODS

Morpholinos and mRNA injections

Antisense morpholino oligonucleotides (MO) targeting the Ovo1 translation start site (Ovo1 ATG MO), Ovo1 5′ untranslated region (Ovo1 5′UTR MO) and Rab11fip2 exon2 splice-donor site (Fip2 MO) were purchased from Gene Tools and dissolved in 1× Danieau's buffer for injection (see Table S2 in the supplementary material). The Ncad MO was described previously (Lele et al., 2002). To test the efficacy of Ovo1 MOs, the target sequences were fused to Gfp, subcloned into pCS2+ to synthesize capped mRNA (mMessage mMachine Kit, Ambion), and co-injected with or without Ovo1 MO into 1- to 4-cell-stage embryos and assayed for Gfp expression. Ovo1 5′UTR MO was most effective and used for all subsequent experiments (Ovo1 MO). Fip2 MO efficacy was assayed by RT-PCR to detect alternatively spliced products. For single MO experiments, 3 ng of Ovo1 MO, 2 ng p53 MO, 0.75-3 ng Fip2 MO and 1 nl of a 50 μM solution of Ncad MO were injected into 1- to 4-cell-stage embryos. For genetic interactions studies, the amount of each MO injected was decreased by half. For rescue experiments, the full-length open reading frame (ORF) of *ovo1* was cloned into the pEGFP:C3 vector and subcloned into pCS2+ to generate a *gfp:ovo1* fusion construct. *gfp:ovo1* mRNA (85 pg) was injected at the 1-cell stage.

To study Ncad subcellular localization, 1-cell-stage embryos were injected with 5-50 pg of linearized *ncad:gfp* plasmid (Jontes et al., 2004) and then photographed at 8-10 hours post-fertilization (hpf) with a Zeiss META 510 confocal microscope.

For *rab11fip2* overexpression studies, the full-length ORF was cloned into *Xho*I sites of pCS2+ (see Table S3 in the supplementary material) and verified by sequencing with T7 and SP6. *rab11fip2* mRNA was co-injected with 100 pg *mCherry* mRNA as a tracer into *sox10(7.2):gfp* transgenic embryos and photographed using a Zeiss Axioplan 2 microscope.

Heat-shock experiments

To test responses of genes (*ovo1*, *rab3c*, *rab12*, *rab11fip2*, *sec6*) to Wnt signaling, heterozygous *Tg(hs:dnTcf-GFP)w26*$^{+/-}$ males were outcrossed to wild-type females (Lewis et al., 2004). Transgenic embryos at 13 hpf were heat-shocked for 1 hour at 37°C and immediately transferred to embryo medium at room temperature. Gfp-positive (dnTcf3 transgenics) and Gfp-negative (wild type) controls were immersed in Trizol reagent 30 minutes post-heat-shock for *ovo1* expression studies or 2 hours post-heat-shock for *rab3c*, *rab12*, *rab11fip2* and *sec6* expression studies, and mRNA was isolated for qPCR (see below).

For rescue experiments, fertilized eggs of *Tg(hs:dnTcf-GFP)w26* heterozygotes (in similar wild-type outcrosses) were injected with mRNA encoding a *gfp:ovo1* fusion protein and similarly heat-shocked at 10 hpf. Embryos were fixed 30 minutes after heat-shock and processed for gene expression by in situ hybridization.

Cell transplantation

Cells were grafted at gastrula stages from *sox10(7.2):gfp* transgenic donors into non-transgenic hosts. Cells were co-transplanted from control donors (injected with 2 ng of p53 MO to prevent MO-induced apoptosis) and *rab11fip2*-overexpressing donors were co-injected with 1.5 ng Ovo1 MO and 2 ng p53 MO (Fig. 7F,G) into wild-type hosts, or in some cases *rab11fib2* mRNA, Ovo1 MO and p53 MO-injected cells were grafted alone (Fig. 7H-M). Embryos were selected based on NC-specific *sox10(7.2):gfp* expression and photographed at 24 hpf.

RNA in situ hybridization and immunohistochemistry

Wholemount RNA in situ hybridization was performed as previously described (Thisse et al., 1993). *ovo1* (GenBank accession number CN021344) was subcloned into *Eco*RI and *Not*I sites of pCS2+ and T3 RNA polymerase was used for probe synthesis. Probes used for NC cell analysis included *sox10*, *mitfa*, *gch*, *dlx2a*, *foxd3* and *mbp* (Knight et al., 2003). *rab3c*, *sec6* and *rab11fip2* were TOPO-cloned using primers listed in Table S3 in the supplementary material. For *rab12*, the predicted ORF was directionally cloned into pCS2+ and T7 RNA polymerase was used for probe synthesis.

To detect Ncad:Gfp, we performed wholemount immunohistochemistry using an anti-Gfp primary antibody (1:1000, Abcam) followed by an anti-rabbit IgG secondary antibody conjugated to Alexa Fluor488 (1:1000, Molecular Probes Invitrogen). Briefly, embryos were washed in PBT (phosphate buffer with 0.1% Tween 20) after overnight fixation in 4% paraformaldehyde and blocked with 5% goat serum for at least 1 hour at room temperature. Incubations with primary and secondary antibodies were performed overnight at 4°C with extensive washing in PBT in between.

Genotyping of *pac*$^{par2.10}$ mutants

To test genetic interactions between *ncad* and either *ovo1* or *rab11fip2*, *parachute*$^{par2.10}$ (*pac*$^{par2.10}$; *ncad*) heterozygotes were first outcrossed to *sox10(7.2):gfp* transgenics, to label the NC cells in live embryos, and injected with subthreshold amounts of Ovo1 MO or *rab11fip2* sense RNA. Individual embryos were separated based on phenotype and mRNA was extracted for subsequent RT-PCR genotyping as previously reported (Lele et al., 2002) using *pac*$^{par2.10}$ sense and antisense primers (Table S3 in the supplementary material). Briefly, a 266 bp *ncad* transcript appears in wild-type siblings, whereas *pac*$^{par2.10}$ heterozygous mutants exhibit additional larger and smaller bands (see Fig. S4 in the supplementary material).

Microarrays

Total RNA from control and Ovo1 morphant, *sox10(7.2):gfp* transgenic embryos was isolated using Trizol reagent (Gibco/BRL) from 12 hpf embryos, when morphants first show NC defects. Experiments were performed in triplicate. RNA samples were processed as per manufacturer's instructions (Affymetrix GeneChip Expression Analysis Technical Manual, Affymetric, Santa Clara, CA, USA). cRNA was hybridized to probe sets present on an Affymetrix GeneChip Zebrafish Genome Array at the MicroArray Facility at UCI. The results were quantified and analyzed using Expression Console ver.1.1 software (Affymetrix) using the PLIER algorithm default values. Microarray gene expression was further analyzed using the DNASTAR ArrayStar program, Version 2.0.0, build 61

(Madison, WI, USA), selecting for genes with a 2-fold or greater difference between samples. Microarray data are available at GEO with accession GSE21529.

Quantitative real time PCR

Total RNA was isolated from embryos using Trizol reagent (Gibco/BRL). First strand cDNA synthesis was performed on 1 μg of total RNA using oligo dT primers and Superscript III reverse transcriptase (Invitrogen). Quantitative real time RT-PCR (qPCR) was performed using the SYBR Green PCR mix (Roche Applied Science) in a DNA Engine Opticon continuous fluorescence detection system (MJ Research) using the qPCR primer sets in Table S3 in the supplementary material.

All samples were quantified by the comparative cycle threshold (Ct) method for relative quantification of gene expression, normalized to *ef1a* (Livak and Schmittgen, 2001). Differences between two groups were analyzed using a two-tailed Student's *t*-test assuming unequal variances.

Chemical treatments

For Brefeldin A (BFA) experiments, *sox10(7.2):gfp* transgenic and/or Ovo1 morphant embryos at 10-11 hpf were treated with 1 μM BFA (initially dissolved in 100% ethanol) in embryo medium (4% dimethyl sulfoxide, DMSO) overnight at 28.5°C. For Ncad:Gfp localization studies, morphant embryos at 6 hpf were similarly treated with BFA for 3 hours prior to fixation at 9 hpf. Control embryos were treated identically, but with 4% DMSO alone in embryo medium.

Confocal imaging and movies

For analysis of NC cell migration, NC cells were labeled by the *sox10(7.2):gfp* transgene starting at 12-14 hpf. Transgenic embryos were manually dechorionated, anesthetized with ethyl-m-aminobenzoate methane sulfanate and mounted in 1% agarose in embryo medium on a coverslip. Approximately 70 μm *z*-stacks at 4 μm intervals were captured using a Zeiss LSM510 META confocal fluorescence microscope. Movies were assembled using ImageJ software and converting to Quicktime at 4 frames per second.

RESULTS

Identification and expression of zebrafish *ovo* genes

In *Ovol2* mutant mice, a subset of cranial NC cells fails to migrate (Mackay et al., 2006). To investigate the roles of *ovo* genes in NC development, we isolated two zebrafish *ovo* orthologs, *ovo1* and *ovo3*, by sequence similarity to mammalian *Ovol1* (see Fig. S1A in the supplementary material). Both Ovo proteins contain the four C_2H_2 zinc finger motifs and the nuclear localization signal (NLS; see Fig. S1A in the supplementary material, underlined black and blue, respectively) characteristic of Ovo transcription factors, as well as the 10 amino acid SNAG domain, thought to act as a transcriptional repressor, at the N-terminus (see Fig. S1A in the supplementary material, red box). Phylogenetic analyses suggest that zebrafish *ovo1* is an ortholog of murine Ovol1, with which it shares partial gene synteny (see Fig. S1B in the supplementary material). By contrast, *ovo3* is more distantly related and conserved in pufferfish, *Fugu rubripes*, whereas a clear ortholog of Ovol2 has not been identified. Consistent with a function as a transcription factor, fusions of *ovo1* or *ovo3* to *egfp* (*ovo:egfp*) injected into zebrafish embryos localized to cell nuclei (see Fig. S1C,C′ in the supplementary material). Although we focus here on a functional analysis of *ovo1*, we obtained largely similar results for *ovo3*.

Zebrafish *ovo1* expression was first detected by in situ hybridization after the mid-blastula transition in the enveloping layer (EVL; Fig. 1A), although earlier maternal expression was detected by RT-PCR (see Fig. S2A in the supplementary material). Expression was later restricted to premigratory neural crest (NC) at 10-12 hours post-fertilization (hpf) as well as prechordal plate mesoderm (PCP; Fig. 1B-D). By 15-24 hpf, *ovo1* expression was detected in subsets of migratory NC cells (Fig. 1E,F), otic placodes and in the roof plate of the neural tube (Fig. 1F). By 48 hpf, expression was detected in the pharyngeal arches, particularly in the first and second arches and presumptive neurocranium (Fig. 1G,H). One consistent and potentially interesting feature of *ovo1* mRNA expression was its dynamic localization within cells, not only in the perinuclear cytoplasm, as seen for most mRNAs (Fig. 1A,B,G,H; arrows), but also in punctate foci within cell nuclei (Fig. 1C,D; arrowheads).

Lineage-specific requirements for Ovo in neural crest development

To investigate the functions of Ovo genes in zebrafish we designed antisense morpholino oligonucleotides (MOs) to create functional knockouts or 'knockdowns'. Using the mouse Ovo-like proteins to deduce the translational start site, we targeted a translation-blocking MO to the 5′UTR of Ovo1. To test MO efficacy, we fused *gfp* to the 3′ end of the Ovo1 MO target site (*ovo1 5′utr:gfp)* and co-injected sense mRNA derived from this construct (500 pg) with 3 ng of the Ovo1 MO, which completely eliminated Gfp expression (see Fig. S2B,C in the supplementary material). To test MO specificity, a second MO was targeted to the translational start site, which caused an identical phenotype (data not shown).

In wild-type embryos, *sox10* expression marks migrating NC in stripes on either side of the neural tube at 24 hpf (Fig. 2A; see also Movie 1 in the supplementary material). Injection of 3 ng Ovo1 MO caused groups of *sox10*$^+$ cells to accumulate in the dorsal midline (Fig. 2B; see Movie 2 in the supplementary material). To determine the identities of these midline *sox10*$^+$ cells, we examined markers of different NC lineages. Both *mitfa*, which marks melanocyte precursors (Fig. 2C,D), and *gch*, which marks xanthophore precursors (Fig. 2E,F) (Lister et al., 2006), were detected in the dorsal midline at 28 hpf in Ovo1 MO-injected embryos (morphants) in similar patterns to *sox10*. However, strikingly, we did not detect defects in patterns of *dlx2* (putative skeletal precursors; Fig. 2G,H) or *foxd3* expression (Fig. 2I,J) in

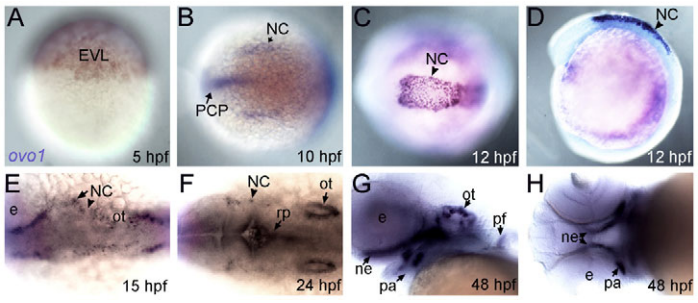

Fig. 1. Expression profile of *ovo1*. Wholemount in situ hybridization. (**A**) Enveloping layer (EVL) expression at 5 hours post-fertilization (hpf). (**B**) Neural crest (NC) and prechordal plate (PCP) expression at 10 hpf (dorsal view, anterior to the left). (**C**,**D**) Expression in premigratory cranial NC cells at 12 hpf (C, dorsal view; D, lateral view). (**E**,**F**) Expression in migrating cranial NC cells at 15 and 24 hpf (dorsal views). Additional expression at 24 hpf in otic vesicles (ot) and roof plate (rp; F, arrows). (**G**,**H**) Expression at 48 hpf in pharyngeal arches (pa), pectoral fins (pf), otic vesicles and neurocranium (ne; G, lateral view; H, ventral view). e, eye.

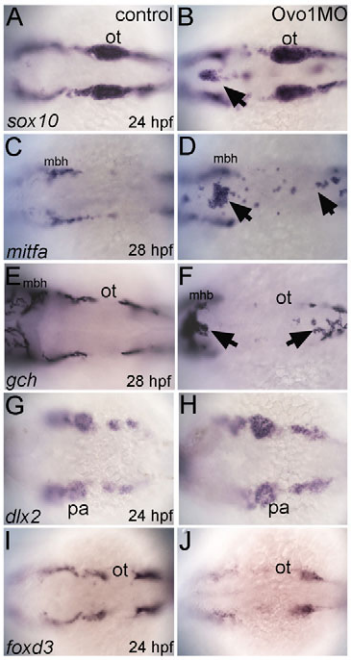

Fig. 2. Ovo1 is required for the migration of NC-derived pigment precursors. Dorsal views, anterior to the left. (**A**,**C**,**E**,**G**,**I**) Controls; (**B**,**D**,**F**,**H**,**J**) Ovo1 morphants. Embryos were processed by wholemount in situ hybridization for expression of *sox10* (A,B), *mitfa* (C,D), *gch* (E,F), *dlx2* (G,H) and *foxd3* (I,J). NC cells migrate in bilateral streams in control embryos (A), but aggregate in the dorsal midline of Ovo1 morphants (B, arrow). Pigment precursors, which express *mitfa* and *gch* at 28 hpf, form ectopic clumps in the dorsal midline in Ovo1 morphants (D,F arrows) when compared with wild-type controls (C,E). However, skeletogenic and glial precursors, which express *dlx2* and *foxd3* at 24 hpf, respectively, do not form clumps in the midline in Ovo1 morphants (G-J). mbh, midbrain-hindbrain boundary; ot, otic vesicle; pa, pharyngeal arches.

Ovo1 morphants, suggesting that defects are restricted to pigment cell lineages. Consistent with these early defects, later numbers of NC-derived melanocytes were strongly reduced in morphants (see Fig. S3A-D in the supplementary material; arrows), whereas jaw morphology appeared normal (see Fig. S3C,D in the supplementary material; arrowheads).

Wnt signaling regulates *ovo1* expression

Pigment cell fate depends on Wnt signaling, and members of the Ovo family are direct Wnt targets in both flies and mice (Li et al., 2002; Payre et al., 1999). Thus, Ovo1 could mediate Wnt signaling during pigment cell fate specification. To address this hypothesis, we analyzed *ovo1* mRNA levels in response to altered Wnt signaling by real-time, quantitative PCR (qPCR). We inhibited Wnt signaling at the transcriptional level using a transgenic line that expresses a truncated, dominant-negative form of Tcf3 (dnTcf3*)* tagged with Gfp under the control of the heat-shock promoter *Tg(hs:dnTcf-GFP)w26*. Embryos were heat-shocked at 13 hpf, bypassing initial requirements for Wnt signaling in NC induction, and transgenic embryos were selected by Gfp expression. As expected, this late heat-shock did not affect initial NC induction, as *sox10*-expressing NC cells were present in both dnTcf3 overexpressing and control embryos (Fig. 3A,B). *ovo1* RNA levels were strongly reduced in embryos overexpressing dnTcf3 when compared with heat-shocked wild-type controls, similar to *axin2*, a direct Wnt target (Fig. 3C). Thus, *ovo1* is a (possibly direct) downstream target of Tcf.

Based on these data, we reasoned that restoring *ovo1* expression in embryos lacking Wnt signaling might rescue NC development. To address this question, we injected a *gfp*-tagged *ovo1* (*gfp:ovo1)* mRNA into a pool of 50% heterozygous *Tg(hs:dnTcf-GFP)w26* and 50% wild-type embryos and performed heat-shock at 10 hpf. This early heat-shock completely eliminated *sox10*-positive NC cells in 45% (25/59) of the uninjected embryos (Fig. 3D; presumably the transgenics) while the rest remained unaffected (*n*=59; Fig. 3E) (Lewis et al., 2004). By contrast, 90% (50/56) of heat-shocked embryos injected with *gfp:ovo1* mRNA showed some *sox10* expression (*n*=56; Fig. 3F,G). Taken together, these data suggest that zebrafish *ovo1* mediates the effects of Wnts, at least in part, on NC formation and pigment cell development.

Genetic interactions between Ovo and N-cadherin

Wnt signaling modulates Ecad, Cad6b and Ncad to regulate NC cell adhesion during EMT and migration. We noticed that our Ovo1 morphants superficially resembled zebrafish *ncad*$^{-/-}$ mutants. Therefore, to elucidate the cellular mechanisms through which *ovo1* genes exert their functions on NC, we focused on possible regulation of adhesion through Ncad.

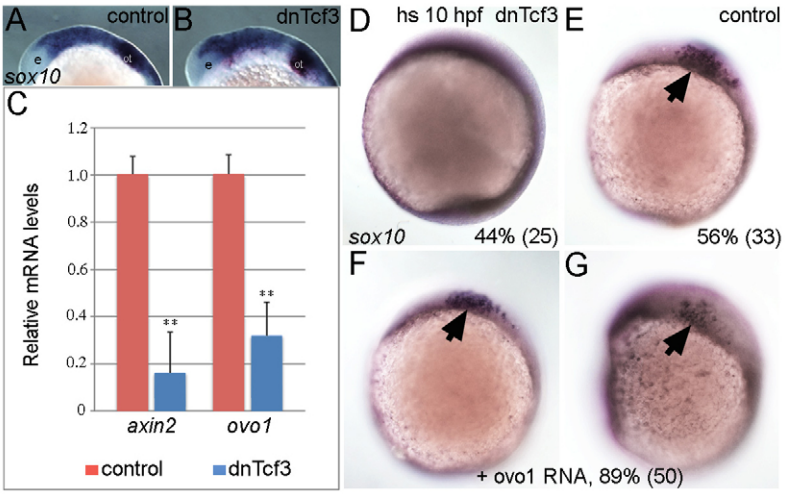

Fig. 3. *ovo1* is induced by Wnt signaling and Ovo1 overexpression partially rescues loss of Wnt signaling in NC cells. (**A**,**B**) *sox10* expression appears identical in controls and embryos overexpressing a heat-shock-inducible form of the dominant-negative form of Tcf3 (dnTcf3), heat-shocked at 12 hpf. e, eye; ot, otic vesicle. (**C**) Real-time PCR shows reduced *ovo1* RNA levels in embryos overexpressing dnTcf3 (blue bars) when compared with wild-type siblings (red bars). Similar reductions occur for *axin2* mRNA, a direct Wnt target. (**D**,**E**) Loss of *sox10* expression in NC in dnTcf3-injected embryos heat-shocked at 10 hpf (D), compared with controls (E, arrow). Percentages in lower right corners indicate phenotype frequency with number of embryos in parentheses. (**F**,**G**) Rescue of *sox10* expression in NC (arrows) in heat-shocked, dnTcf3-injected embryos overexpressing *ovo1* (**, $P \leq 0.01$).

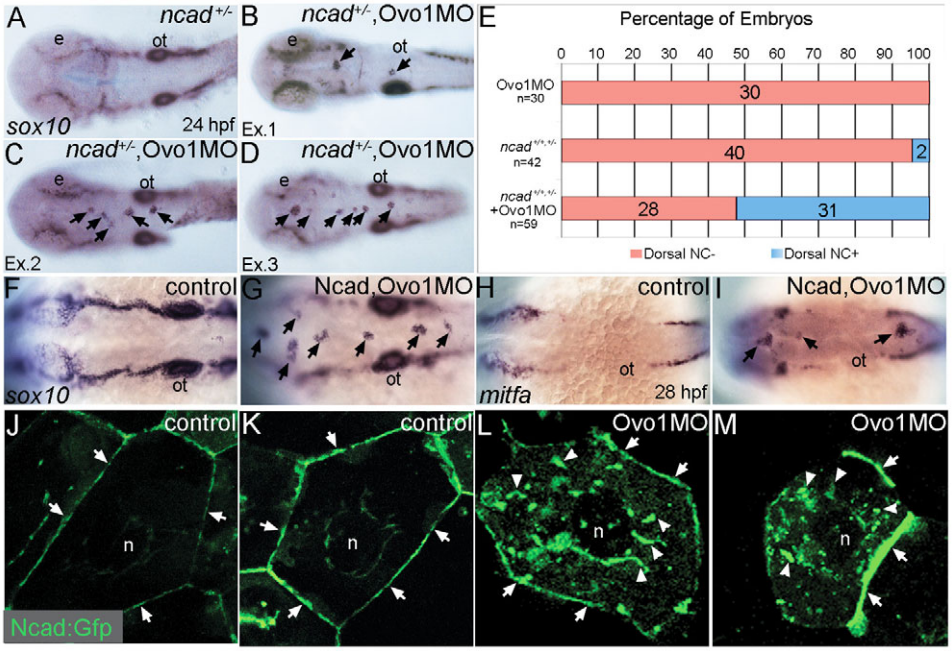

Fig. 4. Interactions between Ovo1 and Ncad. (**A-I**) Ovo1 genetically interacts with Ncad. (A-G) In situ hybridization for *sox10* expression. In both wild types and heterozygous *ncad*$^{+/-}$ mutants (A), *sox10* expression marks bilateral stripes of migrating NC at 24 hpf. Dorsal views, anterior to the left. (B-D) In *ncad*$^{+/-}$ heterozygotes injected with subthreshold levels of Ovo1 MO, a subset of *sox10*-positive NC cells remains at the dorsal midline [arrows; examples (Ex) 1-3]. (E) Quantitation of wild-type (red bars) and ectopic dorsal (blue bars) *sox10*$^{+}$ NC cells. In contrast to controls (F), ectopic *sox10*$^{+}$ cells (G) cluster in the dorsal midline in embryos injected with subthreshold levels of both Ovo1 and Ncad MOs. (H,I) In situ hybridization for *mitfa* expression. In contrast to controls (H), ectopic cells at the dorsal midline express *mitfa* (I, arrows). (**J-M**) Ovo1 regulates Ncad localization. Confocal images of EVL cells in embryos injected with Ncad:Gfp. Ncad:Gfp localizes to the membrane (arrows) and perinuclear region (n, nucleus) of control cells (J,K), whereas Ncad:Gfp accumulates in the cytoplasm of Ovo1 morphant cells (L,M arrowheads). e, eye; n, nucleus; ot, otic vesicle.

To test for genetic interactions between *ovo1* and *ncad*, we injected subthreshold levels of Ovo1 MO into Ncad-deficient embryos. To reduce Ncad levels, we either used heterozygous *ncad*$^{+/-}$ mutants (genotyped as shown in Fig. S4 in the supplementary material) or injected subthreshold levels of Ncad MO, neither of which disrupted NC cells on their own (Fig. 4A,F). *sox10*-positive NC cells formed aggregates in the dorsal midlines of 52.5% (31/59) of *ncad*$^{+/-}$ mutants injected with Ovo1 MO (Fig. 4B-E) and 100% of Ncad/Ovo1 double-morphant embryos (Fig. 4G). Similar results were obtained for *mitfa*-positive pigment precursors (Fig. 4H,I). These results point to a genetic interaction between Ovo1 and Ncad and suggest that they act in a common pathway.

We found significant reductions in *ncad* mRNA levels in Ovo1 morphant zebrafish by qPCR (see Fig. S5A in the supplementary material), but injection of small amounts (~300 pg) of *ncad* mRNA failed to rescue the morphant phenotype (see Fig. S5B-E in the supplementary material). However, this experiment was difficult to interpret because injecting larger amounts of *ncad* mRNA disrupted gastrulation and/or NC migration. These results suggest that reduced *ncad* expression alone cannot account for the Ovo1 loss-of-function phenotype.

Alternatively, Ovo1 might regulate post-translational modifications of Ncad such as its sub-cellular localization. Ncad localization to the tips of filopodia in migratory NC cells is necessary for their proper migration (Monier-Gavelle and Duband, 1995). To address this hypothesis, we used a Gfp-tagged, full-length Ncad (*ncad:gfp*) previously shown to localize to neuronal cell membranes (Jontes et al., 2004). Confocal images of live embryos at gastrula stages revealed *ncad:gfp* at the cell surfaces of epithelial cells of the enveloping layer (EVL; Fig. 4J,K; arrows). By contrast, Ovo1 morphant cells accumulated *ncad:gfp* in punctate structures within the cytoplasm (Fig. 4L,M; arrowheads).

Ovo1 regulates intracellular traffic

How does Ovo1 regulate Ncad localization? We performed a microarray analysis on Ovo1 morphants to identify genes transcriptionally regulated by Ovo1 (see Table S1 in the supplementary material). Interestingly, many of the upregulated genes in Ovo1 morphants encoded proteins involved in cell migration and intracellular vesicle transport. Genes encoding members of the Rab family of GTPases, Rab-interacting proteins, and other secretory pathway components were upregulated more than two-fold. We confirmed this with qPCR for *rab3c*, *rab12*, *rab11fip2* and *sec6*, using *rab25* as an internal control (Fig. 5A).

Surprisingly, we found that *rab3c*, *rab12*, *rab11fip2* and *sec6* were all highly enriched in premigratory NC cells at 12 hpf, the same stage at which we performed the microarray and first detected the Ovo1 morphant phenotype (Fig. 5B-E). At earlier stages, expression of all four genes was ubiquitous throughout the embryo but later became enriched in the NC at 12 hpf and in the dorsal hindbrain and pharyngeal arches at 24-72 hpf (data not shown). Interestingly, we also found significant upregulation of *rab3c*, *rab11fip2* and *sec6* in embryos overexpressing the dnTcf3 transgene when compared with wild-type controls (Fig. 5F). These results suggest that both Wnt and Ovo1 regulate intracellular trafficking pathways, specifically in the NC.

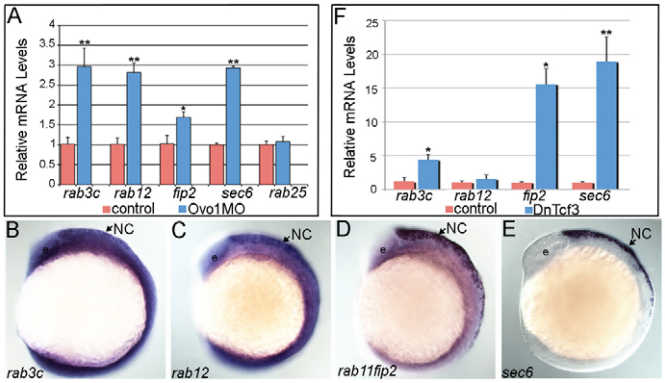

Fig. 5. Ovo1 and Wnt signaling regulate expression of genes involved in intracellular trafficking. (**A**) Real-time PCR in Ovo1 morphants reveals elevated expression levels of *rab3c*, *rab12*, *rab11fip2* and *sec6* mRNA levels (blue bars), compared with controls (red bars), whereas *rab25* levels do not change. (**B-E**) In situ hybridization for expression of *rab3c* (B), *rab12* (C), *rab11fip2* (D) and *sec6* (E) in NC cells (arrows) at 13 hpf. Lateral views, anterior to the left. e, eye. (**F**) Inhibition of Wnt signaling using heat-shock-inducible dnTCF (*Tg(hs:dnTcf-GFP)w26*) increases *rab3c*, *rab11fip2* (indicated as *fip2*) and *sec6* expression (blue bars), but not *rab12*, compared with wild-type siblings (red bars). *, $P \leq 0.05$; **, $P \leq 0.01$.

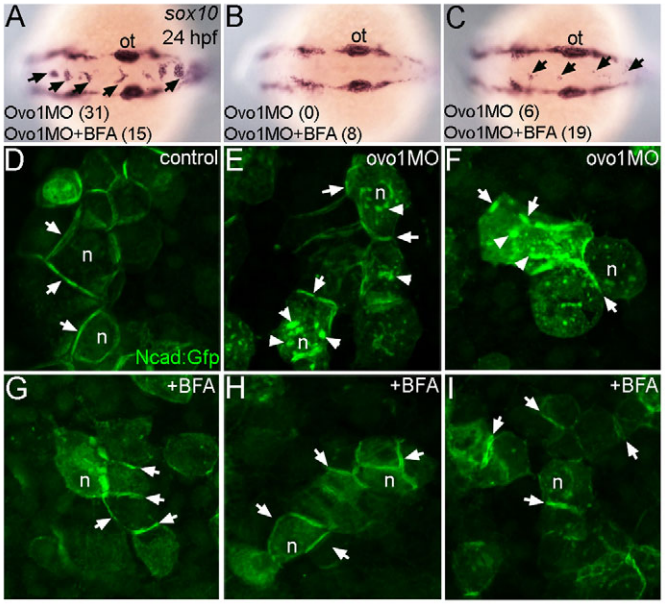

Fig. 6. Inhibition of intracellular trafficking rescues the Ovo1 morphant phenotype. (**A-C**) In situ hybridization for *sox10* at 24 hpf. Dorsal views, anterior to the left. Percentages of embryos with NC cell aggregates at the dorsal midline (arrows) with or without BFA treatment are indicated at the bottom of each panel. (A) A severe example with >5 cells per aggregate over both the midbrain and hindbrain. (C) A less severe example with <5 cells per aggregate exclusively located over the hindbrain. (**D-I**) Ncad:Gfp injections. Ncad:Gfp localizes to the membranes (arrows) of untreated (D) and BFA-treated control cells (G). In Ovo1 morphant cells, Ncad:Gfp also accumulates in the cytoplasm (E,F; arrowheads), but is largely restored to the membrane in BFA-treated Ovo1 morphant cells (H,I). n, nucleus; ot, otic vesicle.

In mice, *Rab3c* regulates neurotransmitter release, whereas *Rab11fip2* belongs to the receptor recycling cascade (Schluter et al., 2004; Somsel Rodman and Wandinger-Ness, 2000) and *sec6* influences both exocytosis and receptor recycling (Langevin et al., 2005). Based on their upregulation in Ovo1 morphants, we hypothesized that suppressing their expression, or the processes they regulate, should at least partially rescue the Ovo1 morphant phenotype. To address this, we used the chemical inhibitor Brefeldin A (BFA), a fungal metabolite that disrupts both endo- and exocytosis via regulation of Golgi complex integrity (Nebenfuhr et al., 2002).

Large aggregates of *sox10*-positive NC cells (>5 cells per aggregate) accumulated in the dorsal midline in most Ovo1-deficient embryos (83.8%, *n*=37; Fig. 6A), while 15% showed a less severe NC defect (fewer than 5 cells per aggregate; 16.2%; Fig. 6C). Treatments of Ovo1 morphants with 1 μM BFA eliminated aggregates either entirely (19.0%, *n*=42; Fig. 6B) or partially (45.2%; Fig. 6C), indicating rescue. BFA treatments also restored the membrane localization of *ncad:gfp* in EVL cells in Ovo1-deficient embryos (Fig. 6H,I), similar to untreated controls or cells treated with BFA alone (Fig. 6D,G), eliminating the intracellular accumulations of *ncad:gfp*$^{+}$ seen in Ovo1 morphant cells (Fig. 6E,F).

Roles for *rab3c*, *rab12* and *rab11fip2* in intracellular trafficking have been studied in vitro but their functions during embryonic development, especially in the NC, have not been described. If elevated levels of one or more of these genes in NC are responsible for the Ovo1 loss-of-function phenotype, then we reasoned that we might be able to phenocopy the Ovo1 morphant phenotype by overexpressing them in early embryos. To address this hypothesis, we injected synthetic mRNA encoding *rab11fip2* and constitutively active forms of *rab3c* and *rab12* (*carab3c* and *carab12*, respectively), together with *mCherry* mRNA to mark injected cells, into transgenic embryos expressing Gfp in NC cells under the control of the *sox10* promoter [*sox10(7.2):gfp*; Fig. 7]. Gfp-positive NC cells migrated normally both in control embryos injected with 100 pg of *mCherry* RNA alone (Fig. 7A) or with different combinations of *carab3c* and *carab12* (data not shown). However, 250 pg of *rab11fip2* alone caused the formation of NC cell aggregates in the dorsal neural tube in 35.3% of injected embryos (Fig. 7B,E) and, similar to Ovo1 morphants, these expressed *mitfa* (see Fig. S6A-C in the supplementary material). However, 90.5% of embryos co-injected with subthreshold levels of both *rab11fip2* mRNA and Ovo1 MO had more severe NC cell aggregates (>5 cells per aggregate), especially at the level of the midbrain, than were observed in single-injected embryos (Fig. 7C-E; arrows), further indicating genetic interactions between the effects of reducing Ovo1 or increasing Rab11fip2 activity.

To corroborate that such defects in migration were autonomous to the NC, we transplanted cells at blastula stages from *sox10(7.2):gfp* transgenics into wild-type embryos. When Ovo1 morphant and wild-type cells were co-transplanted into the same hosts, subsets of *rab11fip2* overexpressing, Ovo1 morphant NC cells (mCherry-positive) failed to migrate and accumulated in the dorsal neural tube (Fig. 7G; arrows), whereas wild-type NC cells (mCherry-negative) migrated normally (Fig. 7F, arrowheads). Similarly, transplantation of *rab11fip2* overexpressing, Ovo1 morphant cells alone resulted in numerous aggregates (Fig. 7H-M; arrows). Taken together, these data suggest that Rab11fip2 modulates NC cell migration.

Is the role of Rab11fip2 in NC cell migration Ncad-dependent? To test this idea, we injected subthreshold levels of *rab11fip2* RNA into heterozygous *ncad*$^{+/-}$ mutants (Fig. 8A,J). In contrast to *ncad*$^{+/-}$ alone, 43.1% (*n*=65) of embryos injected with *rab11fip2*

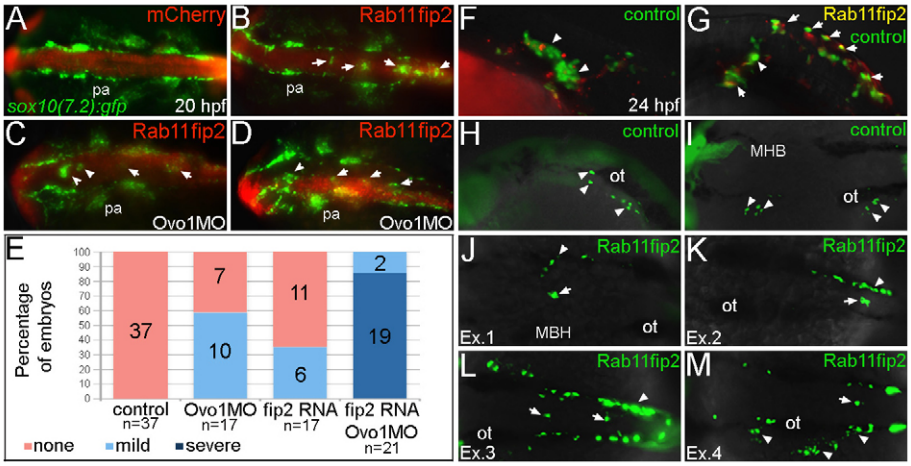

Fig. 7. Overexpression of *rab11fip2* disrupts NC cell migration and exacerbates the Ovo1 morphant phenotype. (**A-E**) *Rab11fip2* and *mCherry* mRNAs were injected into *sox10:gfp* transgenics, in which NC cells fluoresce green in living embryos. Dorsal views, anterior to the left at 24 hpf. (A) Controls injected with *mCherry* mRNA alone show bilateral *sox10:gfp*$^{+}$ cells. (B) By contrast, Gfp-positive cells aggregate in the dorsal midline (arrows) following co-injection of *Rab11fip2* and *mCherry* mRNA. (C,D) Larger aggregates (>5 cells, arrowheads) form over the midbrain in embryos co-injected with subthreshold levels of *Rabfip2* mRNA and Ovo1 MO. (E) Quantitation showing proportions of wild-type (red), mild (pale blue; <5 cells per aggregate located over the hindbrain) and severe (dark blue; >5 cells per aggregate located over both the midbrain and hindbrain) NC defects. (**F-M**) Cell transplantation of *rab11fip2* mRNA-injected cells into wild-type hosts. (F,G) Co-transplantation of *sox10:gfp*, *Rab11fip2*, *mCherry* mRNA-injected (green and red) and *sox10:gfp* uninjected control cells (green) into wild-type hosts; lateral views. *Rab11fip2*-overexpressing cells remain dorsally located (arrows in G). (H-M) Transplantation of control *sox10:gfp*$^{+}$ (H,I) or *Rab11fip2* mRNA-injected *sox10:gfp*$^{+}$ cells (J-M) into uninjected hosts; lateral view (H), dorsal views (I-M). Many *Rab11fip2* overexpressing NC cells remain in the dorsal midline [arrows; examples (Ex) 1-4]. Arrowheads in F-M indicate NC cells that have migrated normally. MHB, mid-hindbrain boundary; ot, otic vesicle; pa, pharyngeal arches.

mRNA displayed ectopic aggregates of *sox10*-positive NC cells in the dorsal midline (Fig. 8B,C,J) that also expressed *mitfa* (Fig. 8G,H). Similar results were obtained when subthreshold levels of *rab11fip2* mRNA and Ncad MO were co-injected (Fig. 8D-F,I,J), demonstrating that Rab11fip2 and Ncad interact genetically and might act in a common pathway.

DISCUSSION

The NC is classically thought to be induced by Wnts and to downregulate Ecad and Ncad in order to exit the neuroepithelium and migrate (Nakagawa and Takeichi, 1995; Nakagawa and Takeichi, 1998). Wnt signaling is also required for NC to form pigment cells but no clear link exists between this and cadherin regulation. The role of Ncad in NC cells is also controversial, as both gain- and loss-of-function disrupt migration (Bronner-Fraser et al., 1992; Nakagawa and Takeichi, 1998; Shoval et al., 2007). Here, we help resolve this debate by suggesting that localization of Ncad to the cell surface is vital for its functions in NC migration and that this is regulated by Wnts. We show that the Wnt target gene, Ovo1, regulates the intracellular trafficking of Ncad, and provide the first evidence for NC-specific functions for intracellular trafficking components, such as *rab11fip2*, in migration (Fig. 9). This might be a more general mechanism by which Wnts control morphogenesis in many contexts.

Our model reconciles several observations (Fig. 9). It agrees with experimental evidence that Ovo1 and Ncad are both required for NC migration. It accommodates data showing that Wnt signaling regulates Ovo1 expression to control Ncad localization. Importantly, it helps explain how defects in Wnt and Ovo1 function disrupt the same subset of NC cells that form pigment cells. This might be the major mechanism by which Wnts control specification and migration of pigment cells and its key feature might be regulated cell adhesion.

Why is Ncad localization important for NC cell migration? These cells need to lose contact with their neighbors during EMT and later establish transient contacts while they pull apart from one another in a process called contact inhibition (Carmona-Fontaine et al., 2008). Ncad localizes to the filopodial tips of migrating NC cells (Monier-Gavelle and Duband, 1995) and, in *Ncad*$^{-/-}$ mutant mouse embryos, NC cells migrate in inappropriate directions (Xu et al., 2001). Thus, rapid turnover of Ncad in different regions of a cell membrane might help it establish transient contacts that allow it to move and guide its path.

Consistent with this idea, we show that many NC cells lose direction in Ovo1-deficient zebrafish embryos and this correlates with reductions in Ncad at the membrane. NC cells end up in ectopic clusters at the roof of the fourth ventricle of the hindbrain or otherwise attach to the neuroepithelium. Cells in Ovo1 morphants show aberrant cytoplasmic accumulation of *ncad:gfp* and rescue of NC cell migration correlates with restoration of cell surface Ncad.

How does Ovo1, a transcription factor, regulate the subcellular localization of Ncad? Our results suggest that among the key transcriptional targets are components of the secretory pathway (including *rab3c*, *rab12*, *rab11fip2* and *sec6*). These are upregulated in Ovo1 morphants and blocking their functions (e.g. with BFA) rescues the morphant phenotype. Surprisingly, all four (*rab3c*, *rab12*, *rab11fip2* and *sec6*) are also normally expressed at high levels, specifically in migrating NC cells. Previous studies have shown requirements for endocytosis and receptor recycling in NC cell motility in vitro (Monier-Gavelle and Duband, 1997). Our results in vivo suggest that *rab3c*, *rab12*, *rab11fip2* and *sec6* function in transport and/or removal of Ncad from the membrane (Fig. 9) and that this is crucial for proper NC migration. Interestingly, Wnt-dependent regulation of *rab11* was recently shown to control tracheal cell intercalation in *Drosophila*;

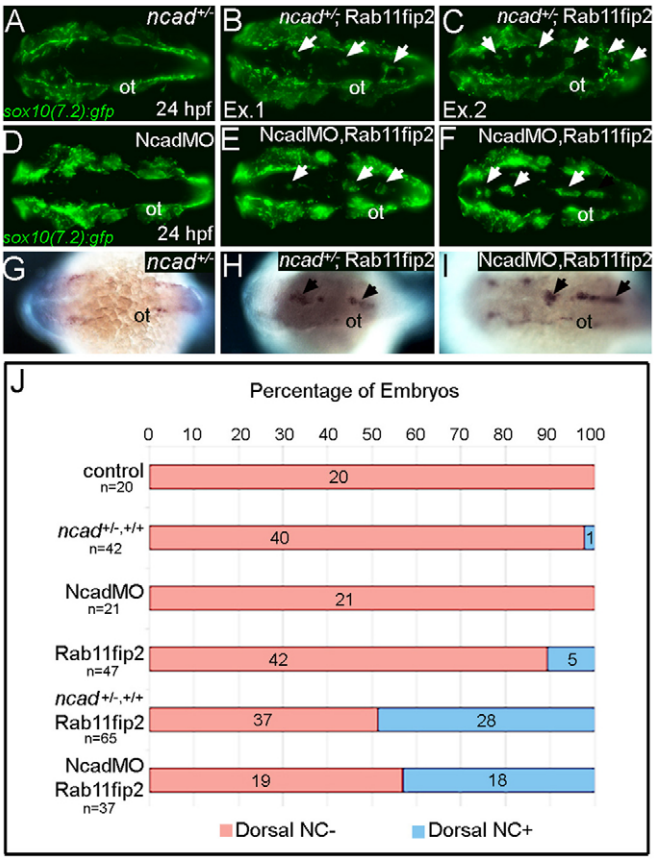

Fig. 8. *rab11fip2* genetically interacts with *ncad* to regulate NC migration. (**A-F**) Live images of *tg:sox10(7.2):gfp* labeling migratory NC cells in *ncad*$^{+/-}$ embryos (A-C) and single Ncad morphants (D-F). In contrast to controls (A,D), Gfp-positive NC cells remain in the dorsal neural tube of *ncad*$^{+/-}$ mutants [B,C; arrows; examples (Ex) 1 and 2] and Ncad morphants (E,F; arrows) injected with subthreshold levels of *Rab11fip2* mRNA. (**G-I**) Similarly, ectopic *mitfa*-positive cells cluster in the dorsal midline (arrows) of *ncad*$^{+/-}$ mutants (H) and Ncad morphants (I) overexpressing *Rab11fip2*, but not in controls (G). (**J**) Quantitation of genetic interaction studies; numbers of embryos with or without ectopic *sox10*$^{+}$ NC clusters in the dorsal midline (blue and red bars, respectively). ot, otic vesicle.

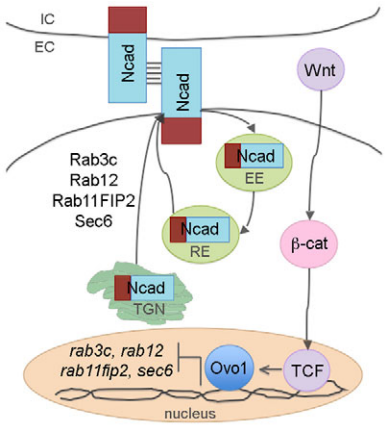

Fig. 9. Model depicting regulation of Ncad trafficking in NC cells by Ovo1. Canonical Wnt/β-catenin signaling through Tcf transcription factors regulates *ovo1* transcript levels in NC cells. Ovo1 normally represses the transcription of *rab3c*, *rab12*, *rab11fip2* and *sec6*, which maintain the balance of intracellular and membrane-localized Ncad. Abnormally high levels of Rab3c, Rab12, Rab11fip2 and Sec6 in Ovo1-deficient NC promote hyperactive intracellular trafficking of Ncad; Ncad secretion from the trans-Golgi network (TGN) and recycling through the early and recycling endosomes (EE and RE) increases. Consequently, Ncad becomes depleted at the membrane. EC, extracellular space; IC, intracellular space.

upregulation of *rab11* in response to Wnt enhanced membrane recycling of Ecad and inhibited cell intercalation (Shaye et al., 2008). Similarly, we find that overexpression of *rab11fip2* in zebrafish is sufficient to restrict the directional migration of NC cells. More than one Rab is probably involved as downregulation of *rab11fip2* alone does not rescue the Ovo1 morphant phenotype (see Fig. S7A-D in the supplementary material).

Ovo1 most likely regulates Ncad transport through the Golgi network, as BFA treatments rescue both the morphant phenotype and the cytoplasmic localization of *ncad:gfp*. BFA causes the trans-Golgi network (TGN) to form a complex with endosomes through its effects on Arf1, a protein that recruits coat proteins of the Golgi complex (Nebenfuhr et al., 2002). Arf1 mutations in yeast disrupt both endo- and exocytic pathways (Gaynor et al., 1998). We find that, at certain concentrations, BFA restores Ncad to the membrane in Ovo1-deficient embryos, rescuing NC migration. BFA was previously shown to restore migration and Ncad localization in avian NC cells (Monier-Gavelle and Duband, 1997). Precisely which aspects of trafficking (endo- versus exocytosis, vesicle recycling, etc.) are most crucial in NC cell migration is an interesting subject for future studies using specific genetic or chemical interventions.

One striking similarity between Ovo1- and Wnt-deficient zebrafish embryos is their specific pigment defect. We hypothesize that the Ovo1- and Wnt-dependent Ncad localization that we have described here promotes migration of NC cells that will form pigment. There are several possible explanations for this lineage-specific requirement. Although widely expressed in the NC at premigratory stages, *ovo1* localizes to a subset of NC cells by 15 hpf, which could be the pigment precursors that fail to migrate in morphants. Alternatively, Ovo1 deficiency might disrupt migration of a random subset of homogeneous NC cells, which subsequently adopt a pigment precursor identity. A subset of NC cells also fails to migrate in *Ovol2*$^{-/-}$ mutant mice, although it is not known if these are also pigment progenitors (Mackay et al., 2006). Intriguingly, NC that forms pigment migrates later than many other populations and this timing might be altered in *Ovo* mutants (Schilling and Kimmel, 1994). Unlike in mice, where NC cells fail to proliferate and die in *Ovol2*$^{-/-}$ mutants (Mackay et al., 2006), in zebrafish we find no changes in proliferation or survival (see Fig. S8A,B in the supplementary material) and cannot rescue defects by inhibiting apoptosis with a p53 MO (see Fig. S8C-J in the supplementary material). Both ectodermal specification and subsequent epidermal differentiation also appear normal (see Fig. S8K-N in the supplementary material). Thus, our results suggest that the effects of Ovo1 on pigment precursors are due to its roles in migration.

The NC has played an important role in the evolution of chordates and is one of the defining characteristics of vertebrate embryos (Gans and Northcutt, 1983). How did this cell population arise during evolution? NC cells originate, at least in part, from the non-neural ectoderm that later forms the epidermis, and relatives of many genes

known to mark NC cells in vertebrates are expressed in this ectoderm in their invertebrate chordate relatives. For example, single *dlx* and *tfap2a* genes in amphioxus, *AmphiDll* and *AmphiAp2*, respectively, are expressed in non-neural ectoderm, suggesting ancestral functions in epidermal development (Holland et al., 1996; Meulemans and Bronner-Fraser, 2002). *Drosophila ovo* acts as a transcriptional switch in the epidermis integrating the Wingless (Wg) and Epidermal growth factor receptor (Der) signaling pathways to induce cytoskeletal changes associated with denticle production, including F-actin bundling and Apc2 localization (Delon et al., 2003; Payre et al., 1999). Similarly, Ovo proteins expressed in the epidermis might have been co-opted during chordate evolution to integrate signaling pathways that control cell shape and movement, leading to the advent of a novel migratory NC cell population.

Acknowledgements
We thank M. Hammerschmidt (*ncad*-MO), R. Brewster (*ncad* mutants), R. Dorsky (*dntcf3* transgenics) and J. Jontes (*ncad:gfp* constructs) for reagents; Dr X. Dai for advice; Drs X. Dai, I. Blitz, K. Cho and M. Waterman for comments on the manuscript; and the Schilling laboratory for help with the manuscript and technical support. Funding for this study was provided by the NIH (R01 NS-41353 and R01 DE-13828) to T.F.S. and an NSF GRF to S.P. Deposited in PMC for release after 12 months.

Competing interests statement
The authors declare no competing financial interests.

Supplementary material
Supplementary material for this article is available at
http://dev.biologists.org/lookup/suppl/doi:10.1242/dev.048439/-/DC1

References
Akitaya, T. and Bronner-Fraser, M. (1992). Expression of cell adhesion molecules during initiation and cessation of neural crest cell migration. *Dev. Dyn.* **194**, 12-20.
Aybar, M. J., Nieto, M. A. and Mayor, R. (2003). Snail precedes slug in the genetic cascade required for the specification and migration of the *Xenopus* neural crest. *Development* **130**, 483-494.
Bronner-Fraser, M., Wolf, J. J. and Murray, B. A. (1992). Effects of antibodies against N-cadherin and N-CAM on the cranial neural crest and neural tube. *Dev. Biol.* **153**, 291-301.
Burstyn-Cohen, T. and Kalcheim, C. (2002). Association between the cell cycle and neural crest delamination through specific regulation of G1/S transition. *Dev. Cell* **3**, 383-395.
Burstyn-Cohen, T., Stanleigh, J., Sela-Donenfeld, D. and Kalcheim, C. (2004). Canonical Wnt activity regulates trunk neural crest delamination linking BMP/noggin signaling with G1/S transition. *Development* **131**, 5327-5339.
Cano, A., Perez-Moreno, M. A., Rodrigo, I., Locascio, A., Blanco, M. J., del Barrio, M. G., Portillo, F. and Nieto, M. A. (2000). The transcription factor snail controls epithelial-mesenchymal transitions by repressing E-cadherin expression. *Nat. Cell Biol.* **2**, 76-83.
Carmona-Fontaine, C., Matthews, H. K., Kuriyama, S., Moreno, M., Dunn, G. A., Parsons, M., Stern, C. D. and Mayor, R. (2008). Contact inhibition of locomotion in vivo controls neural crest directional migration. *Nature* **456**, 957-961.
Dai, X., Schonbaum, C., Degenstein, L., Bai, W., Mahowald, A. and Fuchs, E. (1998). The ovo gene required for cuticle formation and oogenesis in flies is involved in hair formation and spermatogenesis in mice. *Genes Dev.* **12**, 3452-3463.
Delon, I., Chanut-Delalande, H. and Payre, F. (2003). The Ovo/Shavenbaby transcription factor specifies actin remodelling during epidermal differentiation in *Drosophila*. *Mech. Dev.* **120**, 747-758.
Dorsky, R. I., Moon, R. T. and Raible, D. W. (1998). Control of neural crest cell fate by the Wnt signalling pathway. *Nature* **396**, 370-373.
Dorsky, R. I., Raible, D. W. and Moon, R. T. (2000). Direct regulation of nacre, a zebrafish MITF homolog required for pigment cell formation, by the Wnt pathway. *Genes Dev.* **14**, 158-162.
Gans, C. and Northcutt, R. G. (1983). Neural crest and the origin of vertebrates: a new head. *Science* **220**, 268-273.
Gaynor, E. C., Chen, C. Y., Emr, S. D. and Graham, T. R. (1998). ARF is required for maintenance of yeast Golgi and endosome structure and function. *Mol. Biol. Cell* **9**, 653-670.
Holland, N. D., Panganiban, G., Henyey, E. L. and Holland, L. Z. (1996). Sequence and developmental expression of AmphiDll, an amphioxus Distal-less gene transcribed in the ectoderm, epidermis and nervous system: insights into evolution of craniate forebrain and neural crest. *Development* **122**, 2911-2920.
Ikeya, M., Lee, S. M., Johnson, J. E., McMahon, A. P. and Takada, S. (1997). Wnt signalling required for expansion of neural crest and CNS progenitors. *Nature* **389**, 966-970.
Jin, E. J., Erickson, C. A., Takada, S. and Burrus, L. W. (2001). Wnt and BMP signaling govern lineage segregation of melanocytes in the avian embryo. *Dev. Biol.* **233**, 22-37.
Jontes, J. D., Emond, M. R. and Smith, S. J. (2004). In vivo trafficking and targeting of N-cadherin to nascent presynaptic terminals. *J. Neurosci.* **24**, 9027-9034.
Khila, A., El Haidani, A., Vincent, A., Payre, F. and Souda, S. I. (2003). The dual function of ovo/shavenbaby in germline and epidermis differentiation is conserved between *Drosophila melanogaster* and the olive fruit fly *Bactrocera oleae*. *Insect Biochem. Mol. Biol.* **33**, 691-699.
Knight, R. D., Nair, S., Nelson, S. S., Afshar, A., Javidan, Y., Geisler, R., Rauch, G. J. and Schilling, T. F. (2003). lockjaw encodes a zebrafish tfap2a required for early neural crest development. *Development* **130**, 5755-5768.
Langevin, J., Morgan, M. J., Sibarita, J. B., Aresta, S., Murthy, M., Schwarz, T., Camonis, J. and Bellaiche, Y. (2005). *Drosophila* exocyst components Sec5, Sec6, and Sec15 regulate DE-Cadherin trafficking from recycling endosomes to the plasma membrane. *Dev. Cell* **9**, 365-376.
Le Douarin, N. M., Creuzet, S., Couly, G. and Dupin, E. (2004). Neural crest cell plasticity and its limits. *Development* **131**, 4637-4650.
Lele, Z., Folchert, A., Concha, M., Rauch, G. J., Geisler, R., Rosa, F., Wilson, S. W., Hammerschmidt, M. and Bally-Cuif, L. (2002). parachute/n-cadherin is required for morphogenesis and maintained integrity of the zebrafish neural tube. *Development* **129**, 3281-3294.
Lewis, J. L., Bonner, J., Modrell, M., Ragland, J. W., Moon, R. T., Dorsky, R. I. and Raible, D. W. (2004). Reiterated Wnt signaling during zebrafish neural crest development. *Development* **131**, 1299-1308.
Li, B., Mackay, D. R., Dai, Q., Li, T. W., Nair, M., Fallahi, M., Schonbaum, C. P., Fantes, J., Mahowald, A. P., Waterman, M. L. et al. (2002). The LEF1/beta -catenin complex activates movo1, a mouse homolog of *Drosophila* ovo required for epidermal appendage differentiation. *Proc. Natl. Acad. Sci. USA* **99**, 6064-6069.
Lister, J. A., Cooper, C., Nguyen, K., Modrell, M., Grant, K. and Raible, D. W. (2006). Zebrafish Foxd3 is required for development of a subset of neural crest derivatives. *Dev. Biol.* **290**, 92-104.
Livak, K. J. and Schmittgen, T. D. (2001). Analysis of relative gene expression data using real-time quantitative PCR and the 2(-Delta Delta C(T)) method. *Methods* **25**, 402-408.
Mackay, D. R., Hu, M., Li, B., Rheaume, C. and Dai, X. (2006). The mouse Ovol2 gene is required for cranial neural tube development. *Dev. Biol.* **291**, 38-52.
Meulemans, D. and Bronner-Fraser, M. (2002). Amphioxus and lamprey AP-2 genes: implications for neural crest evolution and migration patterns. *Development* **129**, 4953-4962.
Mevel-Ninio, M., Terracol, R. and Kafatos, F. C. (1991). The ovo gene of *Drosophila* encodes a zinc finger protein required for female germ line development. *EMBO J.* **10**, 2259-2266.
Monier-Gavelle, F. and Duband, J. L. (1995). Control of N-cadherin-mediated intercellular adhesion in migrating neural crest cells in vitro. *J. Cell Sci.* **108**, 3839-3853.
Monier-Gavelle, F. and Duband, J. L. (1997). Cross talk between adhesion molecules: control of N-cadherin activity by intracellular signals elicited by beta1 and beta3 integrins in migrating neural crest cells. *J. Cell Biol.* **137**, 1663-1681.
Nakagawa, S. and Takeichi, M. (1995). Neural crest cell-cell adhesion controlled by sequential and subpopulation-specific expression of novel cadherins. *Development* **121**, 1321-1332.
Nakagawa, S. and Takeichi, M. (1998). Neural crest emigration from the neural tube depends on regulated cadherin expression. *Development* **125**, 2963-2971.
Nebenfuhr, A., Ritzenthaler, C. and Robinson, D. G. (2002). Brefeldin A: deciphering an enigmatic inhibitor of secretion. *Plant Physiol.* **130**, 1102-1108.
Oliver, B., Singer, J., Laget, V., Pennetta, G. and Pauli, D. (1994). Function of *Drosophila* ovo+ in germ-line sex determination depends on X-chromosome number. *Development* **120**, 3185-3195.
Payre, F., Vincent, A. and Carreno, S. (1999). ovo/svb integrates Wingless and DER pathways to control epidermis differentiation. *Nature* **400**, 271-275.
Raible, D. W. and Eisen, J. S. (1994). Restriction of neural crest cell fate in trunk of embryonic zebrafish. *Development* **120**, 495-503.
Schilling, T. F. and Kimmel, C. B. (1994). Segment and cell type lineage restrictions during pharyngeal arch development in the zebrafish embryo. *Development* **120**, 483-494.
Schluter, O. M., Schmitz, F., Jahn, R., Rosenmund, C. and Sudhof, T. C. (2004). A complete genetic analysis of neuronal Rab3 function. *J. Neurosci.* **24**, 6629-6637.
Shaye, D. D., Casanova, J. and Llimargas, M. (2008). Modulation of intracellular trafficking regulates cell intercalation in the Drosophila trachea. *Nat. Cell Biol.* **10**, 964-970.
Shoval, I., Ludwig, A. and Kalcheim, C. (2007). Antagonistic roles of full-length N-cadherin and its soluble BMP cleavage product in neural crest delamination. *Development* **134**, 491-501.

Somsel Rodman, J. and Wandinger-Ness, A. (2000). Rab GTPases coordinate endocytosis. *J. Cell Sci.* **113**, 183-192.
Taneyhill, L. A., Coles, E. G. and Bronner-Fraser, M. (2007). Snail2 directly represses cadherin6B during epithelial-to-mesenchymal transitions of the neural crest. *Development* **134**, 1481-1490.
Thisse, C., Thisse, B., Schilling, T. F. and Postlethwait, J. H. (1993). Structure of the zebrafish snail1 gene and its expression in wild-type, spadetail and no tail mutant embryos. *Development* **119**, 1203-1215.
Vallin, J., Thuret, R., Giacomello, E., Faraldo, M. M., Thiery, J. P. and Broders, F. (2001). Cloning and characterization of three *Xenopus* slug promoters reveal direct regulation by Lef/beta-catenin signaling. *J. Biol. Chem.* **276**, 30350-30358.
Xu, X., Li, W. E., Huang, G. Y., Meyer, R., Chen, T., Luo, Y., Thomas, M. P., Radice, G. L. and Lo, C. W. (2001). Modulation of mouse neural crest cell motility by N-cadherin and connexin 43 gap junctions. *J. Cell Biol.* **154**, 217-230.